



This is a repository copy of *The PiGas: a low-cost approach to volcanic gas sampling*.

White Rose Research Online URL for this paper:

<https://eprints.whiterose.ac.uk/211764/>

Version: Published Version

---

**Article:**

Pering, T.D. [orcid.org/0000-0001-6028-308X](https://orcid.org/0000-0001-6028-308X), Wilkes, T.C., Layana, S. et al. (2 more authors) (2024) The PiGas: a low-cost approach to volcanic gas sampling. *Journal of Volcanology and Geothermal Research*, 449. 108063. ISSN 0377-0273

<https://doi.org/10.1016/j.jvolgeores.2024.108063>

---

**Reuse**

This article is distributed under the terms of the Creative Commons Attribution-NonCommercial (CC BY-NC) licence. This licence allows you to remix, tweak, and build upon this work non-commercially, and any new works must also acknowledge the authors and be non-commercial. You don't have to license any derivative works on the same terms. More information and the full terms of the licence here: <https://creativecommons.org/licenses/>

**Takedown**

If you consider content in White Rose Research Online to be in breach of UK law, please notify us by emailing [eprints@whiterose.ac.uk](mailto:eprints@whiterose.ac.uk) including the URL of the record and the reason for the withdrawal request.



[eprints@whiterose.ac.uk](mailto:eprints@whiterose.ac.uk)  
<https://eprints.whiterose.ac.uk/>



## The PiGas: A low-cost approach to volcanic gas sampling

T.D. Pering<sup>a,\*</sup>, T.C. Wilkes<sup>a</sup>, S. Layana<sup>b</sup>, F. Aguilera<sup>b,c</sup>, M. Aguilera<sup>b</sup>

<sup>a</sup> Department of Geography, Winter Street, University of Sheffield, S10 2TN, UK

<sup>b</sup> Millennium Institute on Volcanic Risk Research - Ckelar Volcanoes, Avenida Angamos 0610, Antofagasta, Chile

<sup>c</sup> Departamento de Ciencias Geológicas, Universidad Católica del Norte, Avenida Angamos 0610, Antofagasta, Chile

### ARTICLE INFO

#### Keywords:

Air quality  
Gas sampling instrumentation  
Geochemistry  
Volcanic gases  
Carbon dioxide  
Sulphur dioxide

### ABSTRACT

Instruments which are designed to measure multiple gases are widely used across several industries with a common focus on environmental gas sampling. Reliable instrumentation and gas sensors are therefore vital for the monitoring of air quality in cities and in more challenging scenarios, for example volcanic gas release. However, such instrumentation is commonly expensive and can be difficult to deploy, meaning that large instrument networks - needed to assess spatial air quality differences - is prohibitive. A bespoke do-it-yourself approach can therefore be beneficial. Here, we detail a new instrument, the PiGas, which is modelled on the successful “Multi-GAS” technique (Shinohara, 2005; Aiuppa et al. 2005) for the measurement of carbon dioxide (CO<sub>2</sub>), sulphur dioxide (SO<sub>2</sub>), hydrogen sulphide (H<sub>2</sub>S), and water vapour (H<sub>2</sub>O). Indeed, CO<sub>2</sub> is a common gas of interest yet its measurement at high accuracy can be expensive. We demonstrate a cost reduction to <£500 by adapting parts used from non-air sampling specific industries and through use of a lower-cost and lower-power requirement CO<sub>2</sub> sensor (the CozIR A-H). We demonstrate the versatility of the PiGas for monitoring indoor and outdoor air quality as a diffuse and pumped sensor. We also test the instrument in two extreme volcanic environments at the high altitude Alitar and Volcán Lastarria (Chile). Overall, the instrumentation shows potential for more widespread co-ordinated use to improve spatial sampling distributions in low concentration scenarios as a supplement to higher accuracy and higher precision instruments in volcanic environments.

### 1. Introduction

The ability to detect levels of specific gases in the atmosphere is important for a range of scenarios from air pollution (Chan et al., 2021; Vallero, 2014) and its potential health effects (Brunekreef and Holgate, 2002; Kampa and Castanas, 2008; Tainio et al., 2021), through to volcanic gas sampling (Aiuppa et al., 2005; Edmonds, 2008) and its role in eruption forecasting (Aiuppa et al., 2007). However, the instrumentation to conduct such measurements is often expensive and therefore prohibitive, meaning that large instrument networks are difficult to deploy.

One solution is a do-it-yourself approach to instrument construction which is becoming more common with the accessibility of components. Recent advances have made use of an Internet of Things (IOT) approach (Saini et al., 2021; Unera et al., 2021), and lower-cost off-the-shelf instrumentation such as the Raspberry Pi microcomputer (Sajjan and Sharma, 2021; Zhang et al., 2021) to begin to solve these issues. Despite these advances such sensors come either uncalibrated or with lower accuracy and precision (Gamboa et al., 2023). Recent usage has even

incorporated instrumentation onto Unoccupied Aerial Systems (UAS) for air pollution (Villa et al., 2016) and volcanic scenarios (James et al., 2020) particularly given the need to sample at remote locations, often at altitude (Liu et al., 2019, 2020; Pering et al., 2020; Rüdiger et al., 2018; Stix et al., 2018; Wood et al., 2020).

Commonly, such air quality measurements are made passively, also referred to as “direct”. There are many advantages to this approach, including the generally low power requirements, and the ability to synchronously measure multiple gases or pollutants. Alternatively, a pumped approach, whereby air is drawn across sensors, can be preferable in environments with pollutants that can change proportions rapidly as this allows the sample to be drawn across the sensor directly rather than through diffusion (Pering et al., 2014). There are two core groups of sensors: electrochemical sensors and spectroscopy-based sensors. Electrochemical sensors have a broad range of applications, including the food and medical industries (Mishra et al., 2018; Wang et al., 2008), a wide range of target gases and are commonly cheaper than the alternative spectroscopic approach. Their operation is based on the production of an electronic signal which is directly proportional to

\* Corresponding author.

E-mail address: [t.pering@sheffield.ac.uk](mailto:t.pering@sheffield.ac.uk) (T.D. Pering).

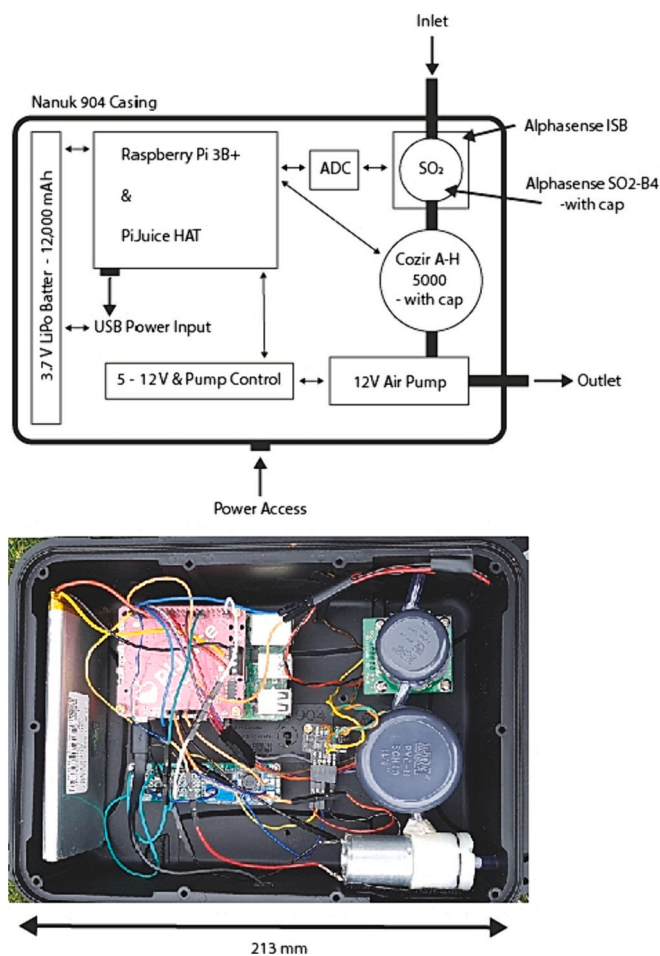


Fig. 1. A schematic of the Pumped PiGas. ISB is Individual Sensor Board. ADC is Analog to Digital Converter.

the amount of the target gas. One of the drawbacks of this approach is that sensor response times (the  $T^{90}$ , time taken for the sensor to register 90% of the real value) can be slow. The spectroscopic approach tends to be faster (commonly non-dispersive infrared – NDIR), given that it is based on characteristic absorption patterns of gas within infrared wavelengths, although this is dependent on exact instrumental setup. Spectroscopic sensors generally come with added cost and is only applicable to gases which absorb in those wavelengths, e.g., carbon dioxide ( $\text{CO}_2$ ).

Here, we test and deploy a new instrument called the “PiGas”, which combines the use of the Raspberry Pi microcomputer and gas sensors, at a cost of <£500. It is designed for use in a range of scenarios, with application to air quality and volcanic gas sampling: direct, pumped, and given low weight (<0.5 kg) could be adapted for UAS mounted sampling. Our approach is modelled after the development of the Multi-GAS analyser, a generally lightweight (<3 kg) and high temporal resolution (~1 Hz) instrument (Aiuppa et al., 2005; Roberts et al., 2012; Shinohara, 2005) which has led to a revolution in the measurement of volcanic gas emissions, but with instrumentation that could be more broadly applied to other scenarios (Kern et al., 2022). Typically, gases measured by Multi-GAS instruments include  $\text{H}_2\text{O}$  (water),  $\text{CO}_2$  (carbon dioxide),  $\text{SO}_2$  (sulphur dioxide),  $\text{H}_2\text{S}$  (hydrogen sulphide), and CO (carbon monoxide). Multi-GAS instruments can come in two forms, one through use of an air pump (pumped) and the other through direct exposure (Roberts et al., 2017; Roberts et al., 2012). There are many major benefits of the Multi-GAS approach including that it is a safer technique to use at logistically challenging sites where access to sources of gas presents hazards, but also that a bespoke approach to the study

Table 1

An itemised list of key components for the construction of the PiGas-Pumped. The PiGas-Direct includes all components except the air pump but included both  $\text{SO}_2$  and  $\text{H}_2\text{S}$ . Note that costs don't include additional peripherals such as wiring and fixing screws. \*Note that the H2S-B4 was incorporated into the PiGas-Pumped for tests at Alitar only.

Item	PiGas-Pumped	Cost
Controller	Raspberry Pi 3B+	£30
$\text{SO}_2$ + ISB	SO2-B4	£100
$\text{H}_2\text{S}$ + ISB	H2S-B4*	N/A
$\text{CO}_2$ , H, T	CozIR® A-H 5000	£120
Pressure	ICP-10125	£15
ADC	ADS1015	£15
Pump	12 V Air Pump	£12
Power	PiJuice HAT	£50
Battery	12,000 mAh	£30
Casing	Nanuk 904	£50
Misc.	Various	N/A
<b>Totals</b>		<b>£423</b>

scenario can be used, although, individual components and construction can be costly meaning that widespread usage is prohibited. In this paper, we detail the construction and testing of the PiGas: an accessible, transferable, and low-cost alternative incorporating the Raspberry Pi. We subsequently evaluate its performance for measuring air quality in Sheffield (UK) and at Alitar and Lastarria volcanoes (northern Chile).

## 2. PiGas instrument overview

Two different setups were configured for the PiGas. Fig. 1 shows the setup of the ruggedised pumped PiGas (*PiGas-Pumped*), designed for handheld use traversing fumaroles or in a fixed position, either temporarily or permanently, the model shown was used for measurements at Lastarria, measurements at Alitar also incorporated a  $\text{H}_2\text{S}$  sensor. The final configuration was a direct exposure PiGas, i.e., with no pump (*PiGas-Direct*). Combining all the elements of the PiGas versions the total cost does not exceed £500 at the time of writing, in each case. See Table 1 for an overview of the parts list.

All versions were controlled by a Raspberry Pi micro-computer, with micro-SD running the operating system, which operated the acquisition code and communication with all sensors. The *PiGas-Direct* and *PiGas-Pumped* both used the Raspberry Pi 3B+. Connection to the PiGas instruments was achieved through wireless protocols and custom written code in Python and MATLAB®. The attached PiJuice HAT (<https://github.com/PiSupply/PiJuice>) acts as an uninterruptible and regulated power supply which allows the operation of the units from installed batteries (see Fig. 1), it is also possible to directly power the units using USB input, e.g., from a portable power bank, simple USB phone charger (supplying at least 5 V, 1A), or a solar panel. The gas sensors are then powered directly from the GPIO (General-Purpose Input-Output) pins on the PiJuice. The 12V air pump (flow rate of 2–3.2 l per minute) was controlled by the Raspberry Pi (on and off) and either powered by a 5V GPIO pin or separate battery power, with subsequent voltage conversion using a custom circuit. The PiGas-Direct and PiGas-Pumped had a 12,000 mAh 3.7V LiPo battery attached to the PiJuice. The chosen target gases for the PiGas were  $\text{CO}_2$ ,  $\text{SO}_2$ ,  $\text{H}_2\text{S}$ , and  $\text{H}_2\text{O}$ , as they are pertinent to both environmental and volcanological monitoring.

### 2.1. CozIR $\text{CO}_2$ sensor

$\text{CO}_2$  is a key gas of interest in several applications, including indoor air quality (Ahmed Abdul-Wahab et al., 2015; Zhang and Srinivasan, 2020), for atmospheric composition monitoring (Keeling et al., 2005), and in certain pollution scenarios, e.g., volcanic emissions (Werner et al., 2019). Measurement of  $\text{CO}_2$  levels is therefore of particular interest. High precision and accuracy instruments are preferable but not always feasible in terms of cost, e.g., a common sensor used is the

**Table 2**  
Manufacturer quoted performance of the SO<sub>2</sub>-B4 and H<sub>2</sub>S-B4 sensors.

Performance Characteristic	SO <sub>2</sub> -B4	H <sub>2</sub> S-B4
T <sub>90</sub> , 0 to 2 ppm	<60 s	<60 s
Noise	5 ppb	1 ppb
Zero drift	<±20 ppb/year	<±100 ppb/year
Sensitivity drift	<±15% year	<20% year
Sensitivity of 2 ppm at -20°C	70–90% of output	77–90% of output
Sensitivity of 2 ppm at 50°C	90–110% of output	100–110% of output

Edinburgh Sensors Gascard NG 0–5000 ppm which costs >£800 (personal quotation from Edinburgh Sensors), higher than the total proposed cost of the PiGas system.

Here we use the CozIR® A-H 5000 (Gas Sensing Solutions) or CozIR® A-H 10000 (these are identical except maximum CO<sub>2</sub>, 5000 ppm and 10,000 ppm respectively) which connects to the Raspberry Pi via Serial UART (Universal Asynchronous Receiver/Transmitter). Their lower powering requirements, 3.3–5.5V (<1.5 mA at 3.3V), make them perfect for use with the Raspberry Pi, with readings possible at 1 Hz. The CozIR® A-H sensors also incorporate temperature (T°C) and relative humidity (RH) allowing the calculation of H<sub>2</sub>O.

Where the sensor may be moving, particularly with altitude, a pressure correction should be applied, which involves the incorporation of a separate pressure sensor, here we use the ICP-10125 Air Pressure Sensor (manufactured by Pimoroni). This can then be incorporated as per Roberts et al. (2018) where P is pressure in hPa:

$$[H_2O_{(g)}] = 6.1121 \times (1.0007 + 3.46 \times 10^{-6} \times P) \times \text{Exp} \left[ \frac{17.502 \times T}{240.97 + T} \right] \times 10^4 \times RH \times P^{-1}$$

All CO<sub>2</sub> measurements were compensated for altitude, where applicable, using the following:

$$CO_2 \text{ corrected} = \frac{CO_2 \text{ original}}{1 + Y(1013 - P)}$$

where Y is the correction factor – 0.000987.

The CozIR® sensors use NDIR and come with manufacturer calibration. The sensor also incorporates in-built autocalibration (with alterable properties) based on exposure to fresh air at 400 ppmv, however, there are also functions which allow user-defined CO<sub>2</sub> values, ideal for calibration using known values or adjustment using current atmospheric CO<sub>2</sub> levels. Detailed sensor specifications and response characteristics are available on the manufacturer's website ([www.gassensing.co.uk](http://www.gassensing.co.uk)). Relative humidity has a range and accuracy of 0–95% and ±5%, respectively. Temperature has a range and accuracy of 0 to 55°C and ±1°C, respectively. For CO<sub>2</sub> the sensor has a manufacturer quoted accuracy of ±50 ppm (±3%) with a resolution of 1 ppm, and operating conditions of 0–50°C, 0–95% RH, and 50–4000 kPa. By default, the sensor outputs a digitally filtered signal (low pass filter, 4 s), however, raw data can also be accessed. Increasing the length of the filter effects the T<sub>90</sub> (time to 90% of actual CO<sub>2</sub> level) and hence would dampen any rapid peaks in CO<sub>2</sub>. However, given the level of sensor noise, a digital filter is required and can be applied post data collection (parameters

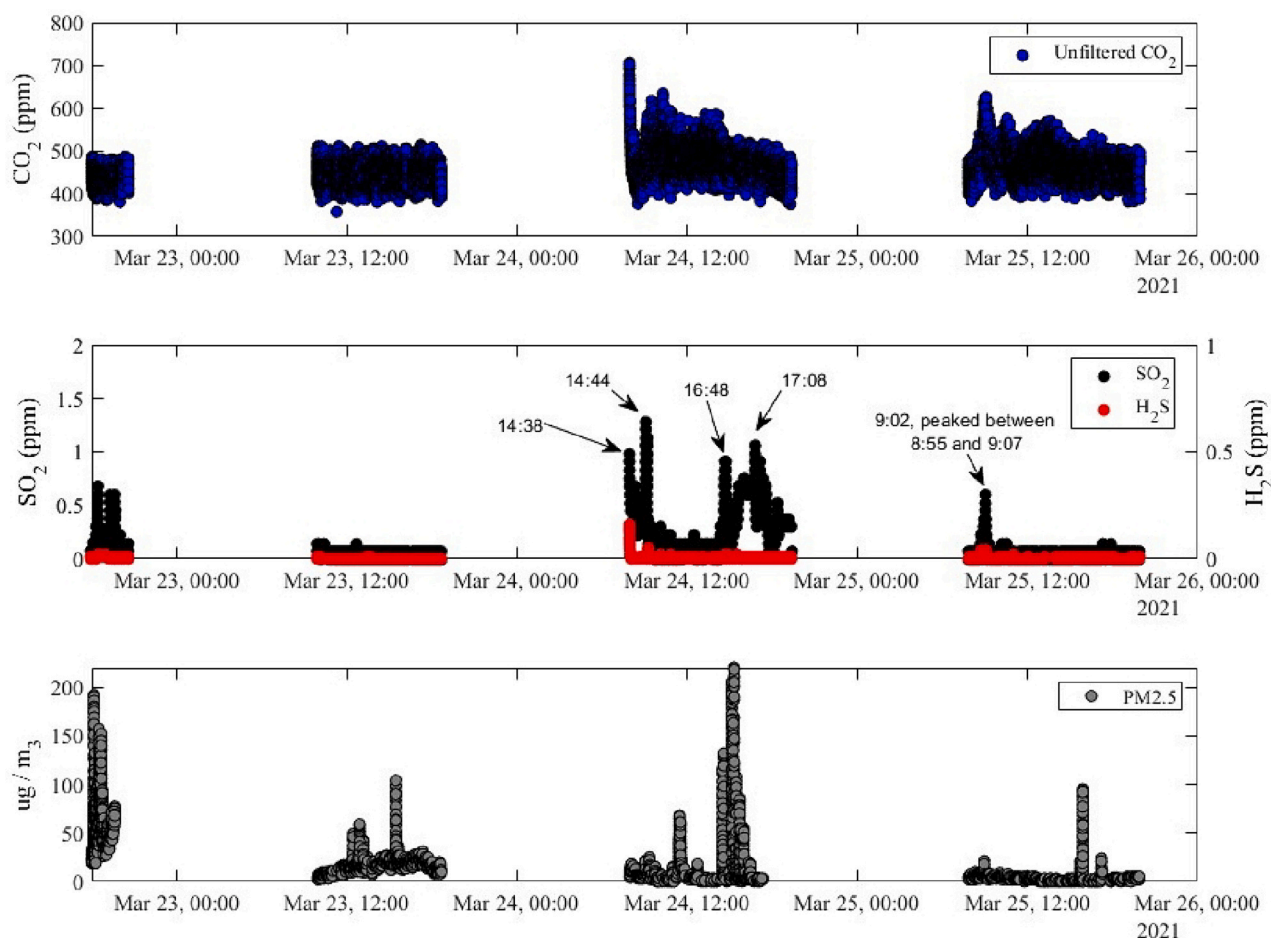


**Fig. 2.** The results of a test of the PiGas-Direct across four days, data gaps are where instruments were turned off. There are clear periods on 24/03/21 of elevated pollution across Sheffield.

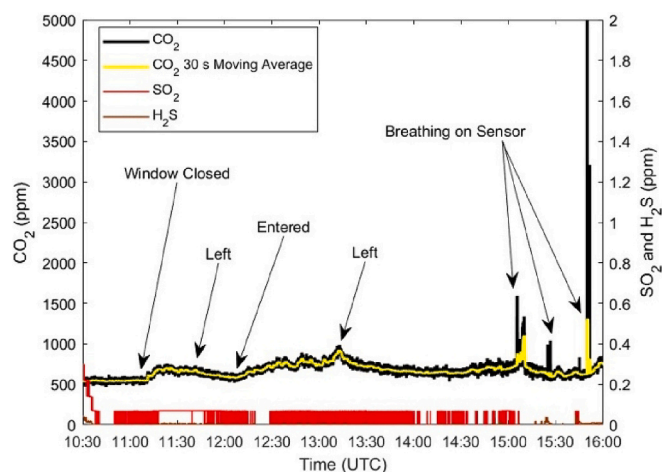


**Fig. 3.** The results of a test of the *PiGas-Pumped* on indoor air quality for an enclosed room with one occupant. Indicated are times when the window was closed and the occupant “Entered” the room, alongside breathing onto the sensor. Note that the changes in  $\text{SO}_2$  level are related to a digital precision issue whilst recording the data.

dependent on the installation setting).

## 2.2. Alphasense $\text{SO}_2$ and $\text{H}_2\text{S}$ electrochemical sensors

$\text{SO}_2$  and  $\text{H}_2\text{S}$  were measured using Alphasense  $\text{SO}_2\text{-B4}$  and  $\text{H}_2\text{S-B4}$  electrochemical sensors. Each gas sensor was attached to an ISB (Individual Sensor Board). The ISB supplies power to the sensor via the Raspberry Pi (3.5–6.4V at 1 mA) ideal for low power applications. Given that the PiJuice regulates powering of the Raspberry Pi, the ISB is provided with stable input providing low noise in the measured signal (manufacturer quoted 5 ppb). The voltage output of the ISB is then passed to an Analog-Digital converter (ADS1015) which is then read via I2C (Inter-Integrated Circuit) communication on the Raspberry Pi. General operating conditions of both  $\text{H}_2\text{S}$  and  $\text{SO}_2$  sensors are: temperatures  $-30\text{--}50^\circ\text{C}$ , relative humidity 15–90%, and pressure 80–120 kPa, although with the latter there are no known issues down to 70 kPa (Roberts et al., 2017). Alphasense sensors come with manufacturer provided calibrations, a summary of sensor performance is provided in Table 2. Full response characteristics and cross-sensitivity details are available on the manufacturer’s website ([www.alphasense.com](http://www.alphasense.com)). Alphasense provide a range of sensors, the *PiGas* has been designed to allow flexibility in target gases in a plug and play approach.

## 3. Results and analysis

Here, we highlight the performance of the *PiGas* versions across air pollution, indoor air quality, and volcanic scenarios to highlight the versatility of the instrumentation.

### 3.1. *PiGas-direct* application: air pollution in sheffield

The *PiGas-Direct* was operated outdoors in a residential area in Sheffield between 22/03/2021–25/03/2021 (Fig. 2). Alongside  $\text{CO}_2$ ,  $\text{SO}_2$ , and  $\text{H}_2\text{S}$ , an “Enviro+” (<https://github.com/pimoroni/enviropyl-us-python>) collected air pollution data, including  $\text{PM}_{2.5}$ , enabling us to highlight periods of poorer air quality in Sheffield, in general.

For the period 22/03/2021–25/03/2021 there were several instances of elevated  $\text{PM}_{2.5}$ , with prominent peaks at a range of times during the day (Fig. 2). For two of the highest peaks in  $\text{PM}_{2.5}$   $\text{SO}_2$  illustrated clear elevated periods, between 0 and 0.68 ppm on the 22/03/2021 and between 0 and 1.06 ppm on the 24/03/2021. For this latter period  $\text{SO}_2$  was elevated between 14:00 and 19:00 GMT, however,

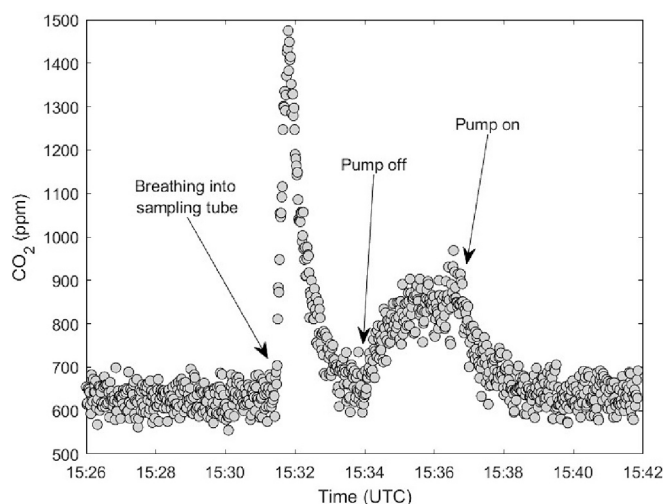


**Fig. 4.** The response characteristics of the *PiGas-Pumped* to breathing into the sampling tube followed by turning the pump off and on again.

$\text{SO}_2$  peaked at 0.98 ppm at 7:55 am and 1.28 ppm at 9 am during periods where  $\text{PM}_{2.5}$  was lower. Note also that the larger spikes in  $\text{SO}_2$  values recorded here are generally short term and lower values are more likely as  $\text{SO}_2$  pollutant data is generally aggregated over 15 min (in air quality monitoring datasets), indeed median values for  $\text{SO}_2$  on all days indicated a value close to 0 ppm (below detection limit of the instrument setup at 0.07 ppm). On 24/04/21 and 25/03/21 peaks in  $\text{SO}_2$  were also present in  $\text{CO}_2$ .  $\text{H}_2\text{S}$  also shows some small peaks in the data, which is likely a result of cross-sensitivity of the sensors. Smaller peaks in  $\text{H}_2\text{S}$  showed potential cross-sensitivities of 4% and 7%. The highest value of  $\text{H}_2\text{S}$  = 0.16 ppm occurred during a peak in  $\text{SO}_2$  of 0.98 ppm which is a cross sensitivity of  $\sim 16\%$ , which may suggest a small proportion of  $\text{H}_2\text{S}$ . Although, all these values are within the manufacturer quoted cross-sensitivity values of  $<20\%$ .

Sheffield has a history of problems with air pollution, including  $\text{SO}_2$  (Garnett, 1980). However, air quality issues related to pollutants such as  $\text{SO}_2$  have abated over time, largely the direct effect of governmental policy decisions (Fowler et al., 2020). The *PiGas-Direct* shows large transient spikes in  $\text{SO}_2$ , likely the result of localised domestic burning, but with background levels commensurate to those reported elsewhere (Wang et al., 2021).

### 3.2. *PiGas-pumped* application: indoor air quality

The *PiGas-Pumped* was operated in an indoor setting to investigate the response characteristics to an indoor air quality scenario. Fig. 3 shows values for  $\text{CO}_2$ ,  $\text{SO}_2$  and  $\text{H}_2\text{S}$  for a period of  $<6$  h in a room with one occupant. Key times and events are highlighted on Fig. 3 including the closing of an open window and when the occupant entered and left the room. The initial drop in  $\text{SO}_2$  levels is related to the initiation of the sensor following instrument start-up.  $\text{SO}_2$  levels then fluctuate slightly, this is the background noise of the instrument setup and an issue with a lower digital precision in the Python code during this earlier test. The response of the sensor to breathing into the sampling tube is measured with commensurately rapid response to changing levels, with a return to ambient concentrations in the room.

The response characteristics and performance of the *PiGas-Pumped* were then further scrutinised by sharply blowing into the sampling tube (Fig. 4). From the peak at  $\sim 1500$  ppm to the baseline ambient  $\text{CO}_2$  of  $\sim 650$  ppm was  $\sim 80$  s. A more progressive change was tested by turning the pump off and on again, on this occasion the peak in  $\text{CO}_2$  of  $\sim 900$  ppm returned to baseline ambient of  $\sim 650$  ppm in  $\sim 60$  s. These results suggest that the *PiGas-Pumped* is able to resolve rapid fluctuations on the order of  $\sim 60\text{--}80$  s dependent on the magnitude of the spike.

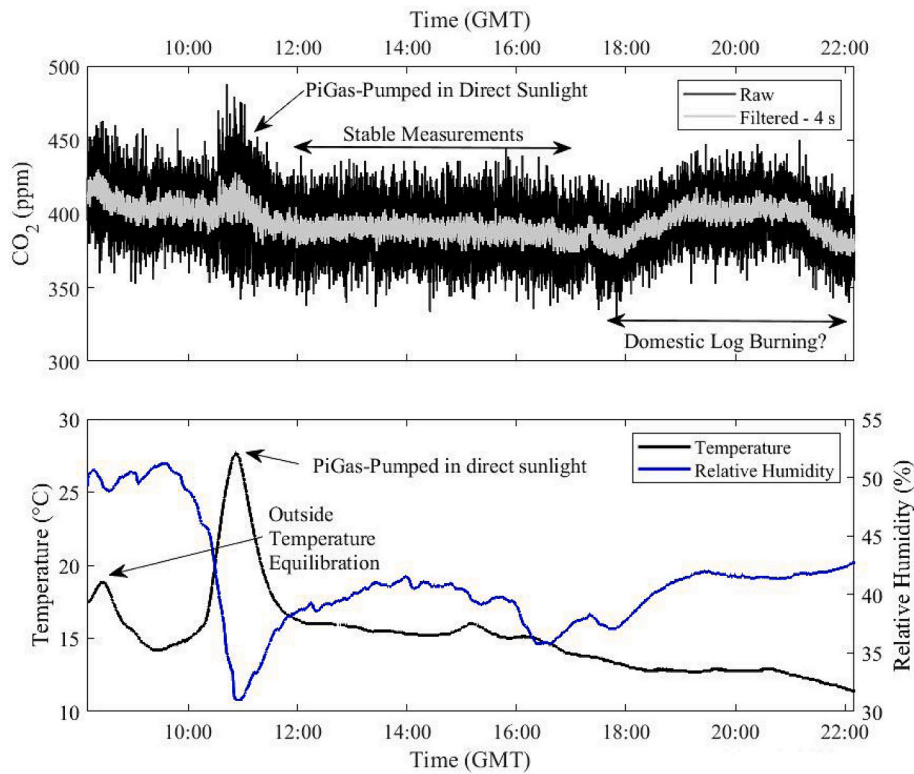


**Fig. 5.** The results of a > 12 h test of the *PiGas-Pumped* showing performance of the CoziR A-H 5000 on 14/03/2022 in Sheffield. For a period of <2 h the *PiGas-Pumped* casing was exposed to direct sunlight causing a large spike in temperature and an associated spike in CO<sub>2</sub>. Also highlighted is an elevated period post 18:00 which could be attributed to an increase in domestic log burning. We also note the slight deviation of CO<sub>2</sub> background values using the CoziR which is likely due to the background air concentration calibration of the sensor.

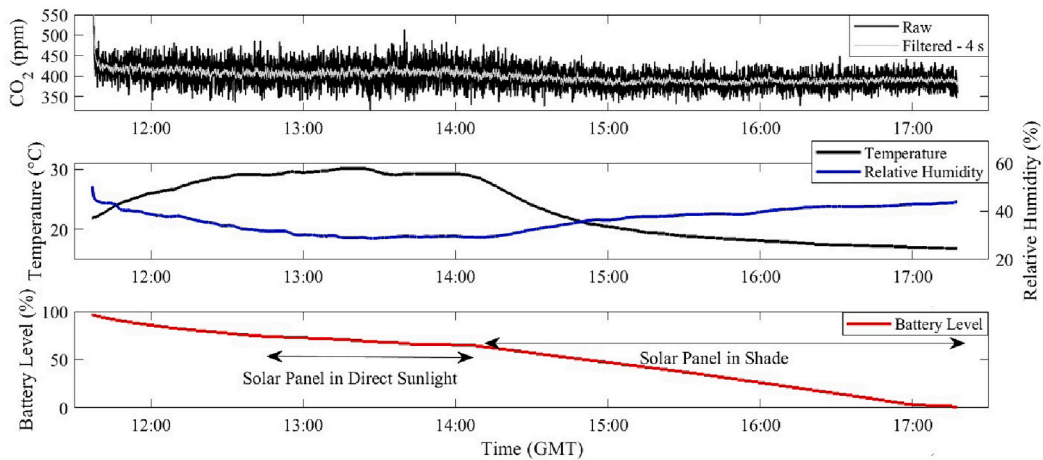


**Fig. 6.** Test of instrument on 18/03/2022 and battery performance with a 12,000 mAh battery installed and attached to a 6 W solar panel during periods in direct sunlight and in shade, with these timeframes clearly visible in the temperature data. CO<sub>2</sub> shows a rapid response to atmospheric air (after inside storage) and a stable level in filtered CO<sub>2</sub> throughout acquisition. °C.

### 3.3. *PiGas-pumped* application: outdoor air quality

The operation of the *PiGas-Pumped* and CO<sub>2</sub> sensor for a period of >12 h outside in Sheffield on 14/03/22 demonstrated the performance of the sensor (continuously USB-mains powered, not from battery), and that where there are rapid changes in temperature, measurement accuracy may be affected. Fig. 5 highlights these responses directly, between 10:00 am and 12:00 pm GMT temperature rapidly increases from ~15°C to ~28°C this is accompanied by an increase in 4 s filtered CO<sub>2</sub> of ~20 ppm and ~50 ppm in raw CO<sub>2</sub>.

Given the low power nature of the *PiGas*, tests for the effect of powering on the *PiGas-Pumped* were conducted to investigate CO<sub>2</sub> sensor response. The *PiGas-Pumped* test on 18/03/22 used a 6 W solar panel between ~12:00 and 5:15 pm (Fig. 6). Vivially, there was no clear response in the CO<sub>2</sub> sensor to the drop in power throughout the day. A rapid response to temperature increase is not seen in comparison to the test on 14/03/2022. However, a moving standard deviation (period 60 s) on this data exhibited in Fig. 7 shows that sensor noise in the raw data is higher during periods of higher temperature (>20°C, 12:00–14:30 pm) than lower temperature (<20°C, 14:30–17:30 pm), with mean

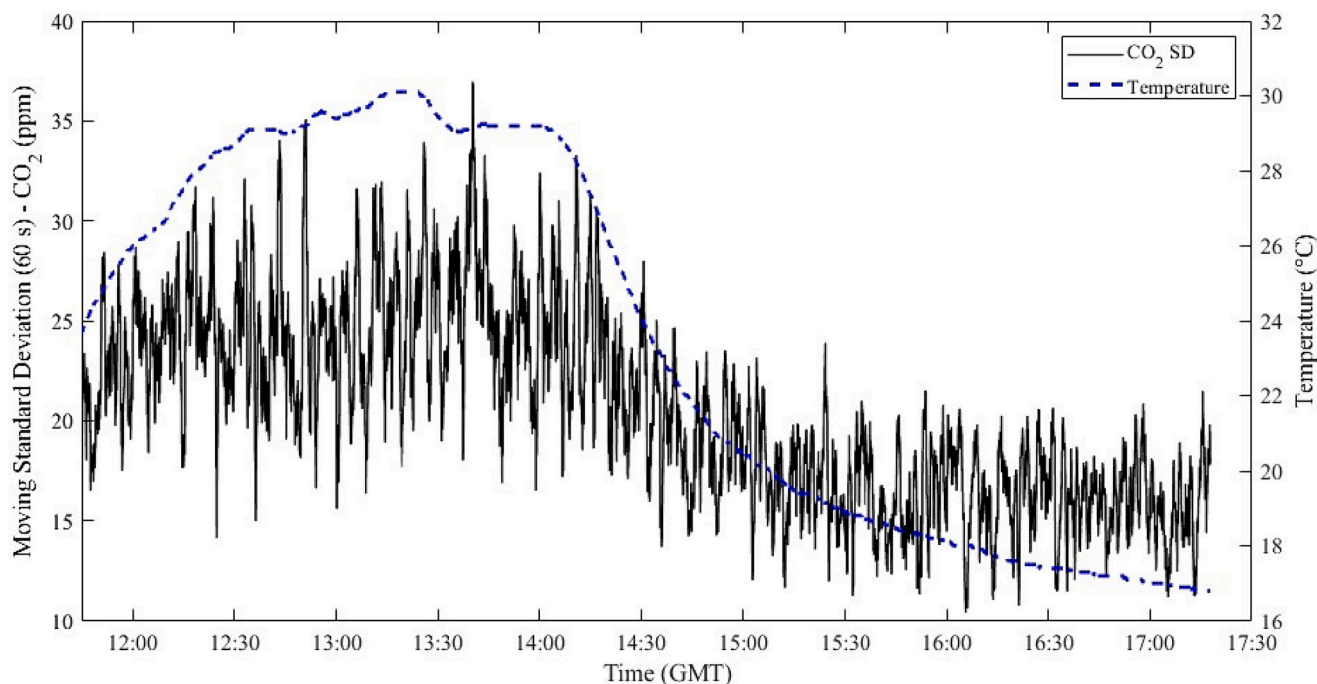


Fig. 7. Standard deviation over a moving 60 s window in CO<sub>2</sub> showing higher standard deviation values leading up to 14:30 GMT.

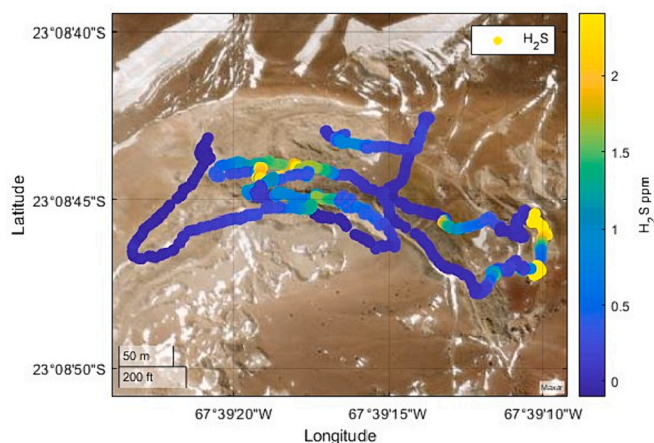


Fig. 8. The transect through the fumarole field at Alitar showing concentrations of H<sub>2</sub>S gas.

standard deviations of  $\pm 24.7$  and  $\pm 16.9$  ppm respectively. At lower temperatures, therefore, sensor accuracy is in line with the manufacturer quoted  $\pm 50$  ppm, at  $\pm 50.7$  ppm. This is also in line with other Multi-GAS instruments, e.g., the PP Systems SBA-5 used by Salas-Navarro et al. (2022), which has an accuracy of  $\pm$  ppm. At higher temperatures, the CozIR, could have a lower accuracy of  $\pm 74$  ppm. Note that changes in background CO<sub>2</sub> as a result of sensor noise are easily correctable in post-processing (Roberts et al., 2017; Tamburello, 2015).

Periods where the solar panel was in direct sunlight allowed the assessment of power consumption. When the solar panel was in direct sunlight each 1%-point drop in battery level took  $\sim 560$  s ( $> 9$  min), corresponding to  $> 14$  h of operation (based on draining 99% of the battery). A test of the PiGas-Pumped on 21/03/2022 with no solar panel confirmed that it ran for  $> 5.5$  h on the battery alone (92% drain over 5.5 h, 215 s per 1%-point drop), again with no clear effect on the CO<sub>2</sub> or any of the sensor response characteristics. Given the relative low power requirements of the instrument, running the instrument for longer periods of time, with larger solar input, could be achieved with ease.

### 3.4. PiGas-pumped: Alitar and Lastarria volcanoes

Alitar volcano, located in Northern Chile in the Central Volcanic Zone of the Andes (CVZA) has persistently active fumarolic activity with a small area of a maar on its flanks (Tassi et al., 2011). At Alitar volcano a version of the PiGas-Pumped was used which incorporated measurements for CO<sub>2</sub>, SO<sub>2</sub>, H<sub>2</sub>S, and H<sub>2</sub>O concentrations on the 2nd March 2023. Fig. 8 shows H<sub>2</sub>S values along the transect conducted of the active fumarolic activity.

Fig. 9a highlights the raw values captured with the PiGas-Pumped across the entire transect at Alitar. Periods within the fumarolic gas are clearly demarcated by spikes in H<sub>2</sub>S concentrations, note that on six occasions the H<sub>2</sub>S sensor was saturated. Nevertheless, there are clear periods where there is matching overlap between all gases measured. Notable periods include 13:30 to 14:00 and 14:15 to 14:25. We highlight one such period in Fig. 9b where the concurrent increases in all gases can be observed, expanding this to show the ratio plots for CO<sub>2</sub>/H<sub>2</sub>S and H<sub>2</sub>O/H<sub>2</sub>S in Fig. 9c and 9d respectively, where all data are raw uncorrected values apart from CO<sub>2</sub> which are 31 s Savitzky-Golay filtered. These results indicate the usability of the CozIR sensor at lower concentrations.

Lastarria volcano, which is part of the Lastarria Volcanic Complex (LVC), is located in Northern Chile in the Central Volcanic Zone of the Andes (CVZA). Lastarria has four persistently active fumarolic fields (Aguilera et al., 2012), which, combined with its high altitude (summit at 5700 m a.s.l.), make it an ideal location to test the limits of the PiGas-Pumped. Note that the purpose of this section is not to make detailed comparisons of volcanic gas compositions, as this is achieved in other papers (Aguilera et al., 2012; Layana et al., 2023; Lopez et al., 2018; Tamburello et al., 2014), but merely to illustrate the potential boundaries of use for this particular setup.

PiGas-Pumped measurements were made for CO<sub>2</sub>, SO<sub>2</sub>, and H<sub>2</sub>O concentrations on 11/05/22 at an average ambient pressure of 54.4 kPa. The bulk plume produced by the lowest altitude fumarole field 1 as per Aguilera et al. (2012) was transected with the results displayed in Fig. 10. Background concentrations of CO<sub>2</sub> and H<sub>2</sub>O were removed from the timeseries using the method of (Tamburello, 2015) to leave the volcanogenic component. This process as per Tamburello (2015)

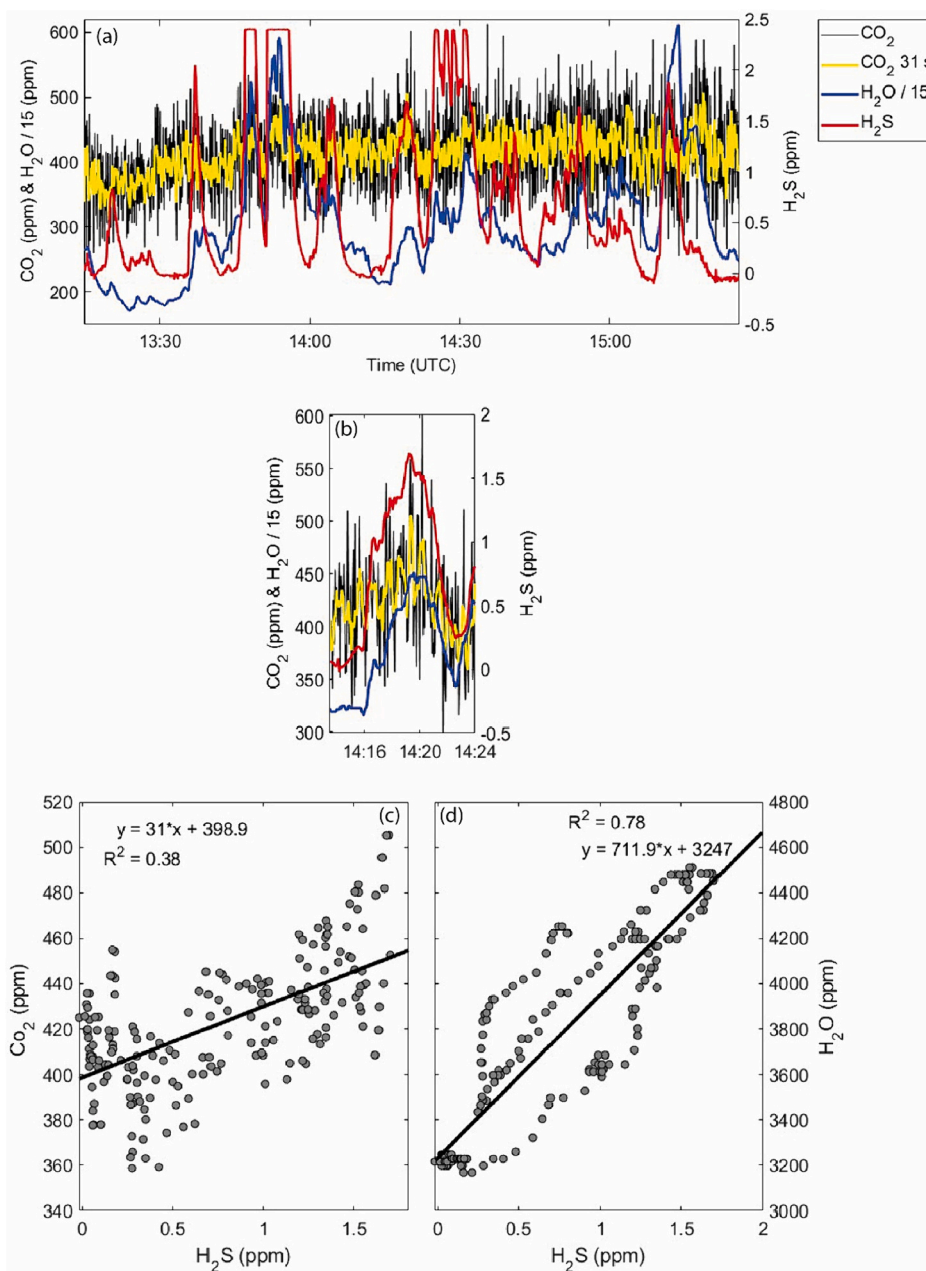


**Fig. 9.** (a) Raw data of all gases during the transect of the fumarole field at Alitar. Note the overlap in peaks between CO<sub>2</sub>, H<sub>2</sub>S, and H<sub>2</sub>O. There are six occasions where H<sub>2</sub>S concentrations saturate the sensor. H<sub>2</sub>O concentrations have been divided by 15 to allow plotting on the same axes. (b) Zoomed and cropped to a period with clear matching peaks, (c) CO<sub>2</sub>/H<sub>2</sub>S scatter plot, where CO<sub>2</sub> has been smoothed by 31 s using the Savitzky-Golay method, R<sup>2</sup> value indicated, and (d) H<sub>2</sub>O/H<sub>2</sub>S scatter plot of raw data, R<sup>2</sup> value indicated.

involved a manual selection of background points and then a smoothing window of 31 s using the Savitzky-Golay method. Given the detection range of the Alphasense sensors, the data used were truncated to the period of data not exceeding 15 ppm where the sensor was saturated in the higher concentrations of the fumarole field.

The results (Fig. 10) show periods where measurements appear to overlap across all gases, for example after 4000 s. There is, however, at points a clear response time difference between the different sensors based purely upon the differences in the peaks of data. This is particular apparent with the large peaks in H<sub>2</sub>O at 1800 s, 4400 s, and 7100 s, which occur prior to peaks in CO<sub>2</sub> and likely represents the differing response times for the incorporated CO<sub>2</sub> of ~30 s T<sub>90</sub> and H<sub>2</sub>O which is ~8 s for T<sub>50</sub> (manufacture value). There is also a delay in SO<sub>2</sub> response, as expected, given the longer T<sub>90</sub> of ~60 s. It is possible that the larger

spikes in H<sub>2</sub>O represent contributions from low temperature fumaroles which are more affected by scrubbing of volcanogenic components (Symonds et al., 2001; Tamburello et al., 2014). To extract comparable gas ratios for future measurements across the gas species would therefore require modelling of the response characteristics of the sensor (Liu et al., 2020; Pering et al., 2020). Furthermore, the challenging climatic conditions and altitude, alongside the difficulty of obtaining a match in contemporaneous datasets indicate that the PiGas may not be best suited to high concentration environments without further development or an alteration in the sensor setup.

#### 4. Discussion

Following the successful approach adapting and designing

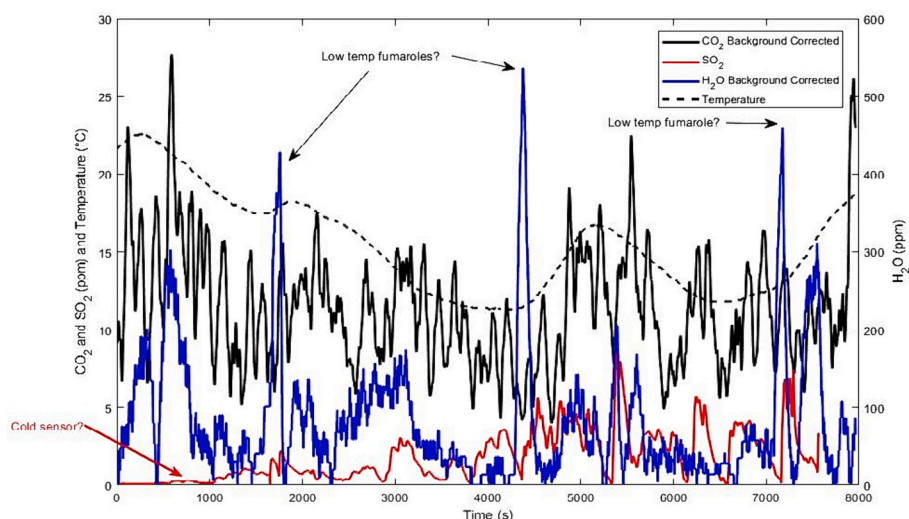


Fig. 10. Results of PiGas-Pumped measurements from transects above fumarole field 1 at Lastarria on 11/05/22.

ultraviolet (UV) cameras for imaging SO<sub>2</sub> using the Raspberry Pi - the “PiCam” (Wilkes et al., 2017; Wilkes et al., 2016) - we use a similar approach for the design of the PiGas. We integrate the use of the transferable Raspberry Pi technology a usable and a low-cost low-power air sampling system, equivalent to the Multi-GAS, demonstrating its use as a cost-effective way of making multi gas species measurements across a range of scenarios. We incorporate the PiJuice HAT (<https://github.com/PiSupply/PiJuice>) which can be used with the Raspberry Pi to enable uninterrupted power supply and recharging in more remote situations using solar panels or low voltage USB input. The PiJuice was used in a successful adaptation of the PiCam (Ilanko et al., 2020; Pering et al., 2020). Previous iterations of Multi-GAS systems have used an Arduino (de Moor et al., 2019; Liu et al., 2020; Rüdiger et al., 2018), which is a micro-controller, rather than the micro-computer setup applied here. To reduce the cost of the instrument there were two main areas of focus: the use of equivalent but lower-cost parts than used in the Multi-GAS (Aiuppa et al., 2005; Roberts et al., 2018; Shinohara, 2005), e.g., through use of components not marketed for use for air sampling (e.g., air pumps used in the medical industry), and the use of a different CO<sub>2</sub> sensor.

For the measurement of SO<sub>2</sub> and H<sub>2</sub>S we used Alphasense sensors. Alphasense electrochemical sensors are not new to air quality or volcanic applications, having been used for air quality (Whitty et al., 2022) and within volcanic plumes or fumaroles previously (Liu et al., 2020; Padrón et al., 2012; Roberts et al., 2018; Roberts et al., 2017; Roberts et al., 2014; Roberts et al., 2012). The performance of the Alphasense sensors is on par with those of City Technology (Roberts et al., 2018) the sensor which is commonly employed in the original Multi-GAS (Aiuppa et al., 2008), although Whitty et al. (2022) do highlight the negative effects of corrosion with direct exposure setups at Masaya volcano.

Overall, we focused on the characteristics of the CozIR-A-H sensor, given its lower cost and powering requirements but lack of detailed characterisation for more challenging measurement conditions, such as for volcanic gases, in the first known volcanic application. We have demonstrated that CO<sub>2</sub> measurements using the CozIR, despite the lower precision and accuracy than other versions of the Multi-GAS (Salas-Navarro et al., 2022) could be useful as a low-cost tool in either a pumped or direct exposure setting. Usage of sensors such as the Gascard NG CO<sub>2</sub> sensors should still be preferred for higher accuracy and precision measurements (Aiuppa et al., 2018). The Gascard NG 0–5000 ppm has a higher sensor accuracy of  $\pm 32.1$  ppm (Honeycutt et al., 2019) than the CozIR, particularly when compared against the  $\pm 74$  ppm at higher temperatures. To mitigate against these lower accuracies the use of filtering can provide more stable measurements with the consequence of

Table 3

A comparison of common sensors used for the measurement of CO<sub>2</sub>. Note this list is meant as illustrative and not an exhaustive list of every sensor available. \*Note that weights of the K30 and Telaire T6615 were not available within manufacture specification documents, values given are a best estimate.

Instrument	Accuracy	T <sub>90</sub> response time	Cost	Weight
Gascard NG 0–5000 ppm	$\pm 2\%$	10 s	>£800	~300 g
Li-830 CO <sub>2</sub>	$\pm 1.5\%$	3.5 s	>£5 k	~1000 g
CozIR® A-H Series	$\pm 3\% / \pm 50$ ppm	30 s	£120	20 g
K30	$\pm 3\% / \pm 30$ ppm	20 s	£100	<100 g*
Telaire T6615	$\pm 75$ ppm	120 s	£80	<100 g*

reducing possible sampling rate and dampening larger peaks in data. However, these differences and mitigations should be balanced against the cost differences, with the CozIR a fifth of the cost and with a large weight difference, 0.3 kg for the Gascard and 0.02 kg for the CozIR. These large reductions in both cost and weight have significant implications for usability and affordability across a range of different settings, with the CozIR family of instruments identified as good targets for UAV applications (Hening et al., 2013), as with this work. Another low-cost sensor, the K30 (Sensair) received a detailed characterisation by Martin et al. (2017) who illustrated accuracies (errors) of ~5 to 21 ppm compared to high calibre research grade sensors, although with higher powering requirements. Table 3 shows a selection of commonly used CO<sub>2</sub> sensors, although a more substantive list can be found in Coulby et al. (2020).

## 5. Summary and implications

Here we detail and test a transferrable, accessible, and low-cost Multi-GAS-style environmental gas sampling unit, the PiGas, costing <£500 across a range of applications related to indoor and outdoor air quality and more extreme volcanic environments. We demonstrate that whilst the PiGas has a lower accuracy than equivalent instruments, particularly with choice of CO<sub>2</sub> sensor, its performance is still comparable to equivalent instruments and when balancing this against cost there are clear benefits. The design of the PiGas could open the technology for use at a wider number of locations than is currently achieved, with the low-cost and weight requirements possibly enabling expanded

use of in airborne scenarios, for example, co-ordinated sampling of multiple sources simultaneously.

### CRedit authorship contribution statement

**T.D. Pering:** Writing – review & editing, Writing – original draft, Software, Methodology, Conceptualization. **T.C. Wilkes:** Writing – review & editing, Software, Methodology. **S. Layana:** Writing – review & editing, Writing – original draft, Methodology, Formal analysis. **F. Aguilera:** Writing – review & editing, Writing – original draft, Resources, Methodology, Funding acquisition, Formal analysis. **M. Aguilera:** Investigation, Formal analysis, Data curation.

### Data availability

Data will be made available on request.

### Acknowledgements

Thomas Wilkes acknowledges the support of a Leverhulme Early Career Fellowship (ECF-2020-107). Tom Pering acknowledges the support of the University of Sheffield. Felipe Aguilera acknowledges FONDECYT Regular 1211220. Felipe Aguilera, Susana Layana and Mauricio Aguilera acknowledge the Millennium Institute on Volcanic Risk Research - Ckellar Volcanoes, ANID Iniciativa Científica Milenio ICN2021\_038. We thank two anonymous reviewers and the two handling editors for their helpful and insightful comments which have greatly improved the manuscript. The authors would further like to thank the organizing committee of the CIGEFU field school for logistics whilst conducting work at Alitar.

### References

- Aguilera, F., Tassi, F., Darrah, T., Moune, S., Vaselli, O., 2012. Geochemical model of a magmatic-hydrothermal system at the Lastarria volcano, northern Chile. *Bull. Volcanol.* 74, 119–134. <https://doi.org/10.1007/S00445-011-0489-5/FIGURES/10>.
- Ahmed Abdul-Wahab, S.A., En, S.C.F., Elkamel, A., Ahmadi, L., Yetilmezsoy, K., 2015. A review of standards and guidelines set by international bodies for the parameters of indoor air quality. *Atmos. Pollut. Res.* 6, 751–767. <https://doi.org/10.5094/APR.2015.084>.
- Aiuppa, A., Federico, C., Giudice, G., Gurrieri, S., 2005. Chemical mapping of a fumarolic field: La Fossa Crater, Vulcano Island (Aeolian Islands, Italy). *Geophys. Res. Lett.* 32, L13309. <https://doi.org/10.1029/2005GL023207>.
- Aiuppa, A., Moretti, R., Federico, C., Giudice, G., Gurrieri, S., Liuzzo, M., Papale, P., Shinohara, H., Valenza, M., 2007. Forecasting Etna eruptions by real-time observation of volcanic gas composition. *Geology* 35, 1115. <https://doi.org/10.1130/G24149A.1>.
- Aiuppa, A., Giudice, G., Gurrieri, S., Liuzzo, M., Burton, M., Caltabiano, T., Mcgonigle, A.J.S., Salerno, G., Shinohara, H., Valenza, M., 2008. Total volatile flux from Mount Etna. *Geophys. Res. Lett.* 35, 2004–2008. <https://doi.org/10.1029/2008GL035871>.
- Aiuppa, A., de Moor, J.M., Arellano, S., Coppola, D., Francofonte, V., Galle, B., Giudice, G., Liuzzo, M., Mendoza, E., Saballos, A., Tamburello, G., Battaglia, A., Bitetto, M., Gurrieri, S., Laiolo, M., Mastroli, A., Moretti, R., 2018. Tracking Formation of a Lava Lake from Ground and Space: Masaya Volcano (Nicaragua), 2014–2017. *Geochim. Geophys. Geosyst.* 19, 496–515. <https://doi.org/10.1002/2017GC007227>.
- Brunekeerf, B., Holgate, S.T., 2002. Air pollution and health. *Lancet* 360, 1233–1242. [https://doi.org/10.1016/S0140-6736\(02\)11274-8](https://doi.org/10.1016/S0140-6736(02)11274-8).
- Chan, K., Schillereff, D.N., Baas, A.C.W., Chadwick, M.A., Main, B., Mulligan, M., O'Shea, F.T., Pearce, R., Smith, T.E.L., van Soesbergen, A., Tebbs, E., Thompson, J., 2021. Low-cost electronic sensors for environmental research: pitfalls and opportunities. *Prog. Phys. Geogr.* 45, 305–338. [https://doi.org/10.1177/0309133320956567/ASSET/IMAGES/LARGE/10.1177\\_0309133320956567-FIG2.JPG](https://doi.org/10.1177/0309133320956567/ASSET/IMAGES/LARGE/10.1177_0309133320956567-FIG2.JPG).
- Coulby, G., Clear, A., Jones, O., Godfrey, A., 2020. A Scoping Review of Technological Approaches to Environmental monitoring. *Int. J. Environ. Res. Public Health* 17, 3995. <https://doi.org/10.3390/IJERPH17113995>.
- de Moor, J.M., Stix, J., Avar, G., Muller, C., Corrales, E., Diaz, J.A., Alan, A., Brenes, J., Pacheco, J., Aiuppa, A., Fischer, T.P., 2019. Insights on Hydrothermal-Magmatic Interactions and Eruptive Processes at Poás Volcano (Costa Rica) from High-Frequency Gas monitoring and Drone Measurements. *Geophys. Res. Lett.* 46, 1293–1302. <https://doi.org/10.1029/2018GL080301>.
- Edmonds, M., 2008. New geochemical insights into volcanic degassing. *Philos. Trans. R. Soc. A Math. Phys. Eng. Sci.* 366, 4559–4579. <https://doi.org/10.1098/rsta.2008.0185>.
- Fowler, D., Brimblecombe, P., Burrows, J., Heal, M.R., Grennfelt, P., Stevenson, D.S., Jowett, A., Nemitz, E., Coyle, M., Lui, X., Chang, Y., Fuller, G.W., Sutton, M.A., Klimont, Z., Unsworth, M.H., Vieno, M., 2020. A chronology of global air quality. *Philos. Trans. R. Soc. A* 378. <https://doi.org/10.1098/RSTA.2019.0314>.
- Gamboa, V.S., Kinast, É.J., Pires, M., 2023. System for performance evaluation and calibration of low-cost gas sensors applied to air quality monitoring. *Atmos. Pollut. Res.* 14, 101645. <https://doi.org/10.1016/J.APR.2022.101645>.
- Garnett, A., 1980. Recent trends in Sulphur dioxide air pollution in the Sheffield urban region. *Atmos. Environ.* 14, 787–796. [https://doi.org/10.1016/0004-6981\(80\)90134-1](https://doi.org/10.1016/0004-6981(80)90134-1).
- Hening, S., Baumgartner, J., Walden, C., Kirmayer, R., Teodorescu, M., Nguyen, N., Ippolito, C., 2013. Distributed sampling using small unmanned aerial vehicles (UAVs) for scientific missions. AIAA Infotech Aerosp. (I A) Conf. <https://doi.org/10.2514/6.2013-4734>.
- Honeycutt, W.T., Ley, M.T., Materer, N.F., 2019. Precision and limits of detection for selected commercially available, low-cost carbon dioxide and methane gas sensors. *Sensors* 19, 3157. <https://doi.org/10.3390/S19143157>.
- Iianko, T., Pering, T.D., Wilkes, T.C., Woitischek, J., D'Aleo, R., Aiuppa, A., McGonigle, A.J.S., Edmonds, M., Garaebiti, E., 2020. Ultraviolet camera measurements of passive and explosive (strombolian) sulphur dioxide emissions at Yasur Volcano, Vanuatu. *Remote Sens.* 12, 2703. <https://doi.org/10.3390/RS12172703>.
- James, M., Carr, B., D'Arcy, F., Diefenbach, A., Dietterich, H., Fornaciai, A., Lev, E., Liu, E., Pieri, D., Rodgers, M., Smets, B., Terada, A., von Aulock, F., Walter, T., Wood, K., Zorn, E., 2020. Volcanological applications of unoccupied aircraft systems (UAS): Developments, strategies, and future challenges. *Volcanica* 3, 67–114. <https://doi.org/10.30909/vol.03.01.67114>.
- Kampa, M., Castanas, E., 2008. Human health effects of air pollution. *Environ. Pollut.* 151, 362–367. <https://doi.org/10.1016/J.ENVPOL.2007.06.012>.
- Keeling, R.F., Piper, S.C., Bollenbacher, A.F., Walker, J.S., 2005. Atmospheric carbon dioxide record from Mauna Loa [WWW Document]. Carbon Dioxide Inf. Anal. Cent. URL <https://cdiac.ess-dive.lbl.gov/trends/co2/sio-mlo> (accessed 2.2.23).
- Kern, C., Aiuppa, A., de Moor, J.M., 2022. A golden era for volcanic gas geochemistry? *Bull. Volcanol.* 84 (43) <https://doi.org/10.1007/s00445-022-01556-6>.
- Layana, S., Aguilera, F., Inostroza, M., Tassi, F., Wilkes, T.C., Bredemeyer, S., González, C., Pering, T.D., McGonigle, A.J.S., 2023. Evolution of the magmatic-hydrothermal system at Lastarria volcano (Northern Chile) between 2006 and 2019: Insights from fluid geochemistry. *Front. Earth Sci.* 11, 513. <https://doi.org/10.3389/FEART.2023.1114001/BIBTEX>.
- Liu, E.J., Wood, K., Mason, E., Edmonds, M., Aiuppa, A., Giudice, G., Bitetto, M., Francofonte, V., Burrow, S., Richardson, T., Watson, M., Pering, T.D., Wilkes, T.C., McGonigle, A.J.S., Velasquez, G., Melgarejo, C., Bucarey, C., 2019. Dynamics of Outgassing and Plume Transport Revealed by Proximal Unmanned Aerial System (UAS) Measurements at Volcán Villarrica, Chile. *Geochemistry. Geophys. Geosystems* 20, 730–750. <https://doi.org/10.1029/2018GC007692>.
- Liu, E.J., Aiuppa, A., Alan, A., Arellano, S., Bitetto, M., Bobrowski, N., Carn, S., Clarke, R., Corrales, E., de Moor, J.M., Diaz, J.A., Edmonds, M., Fischer, T.P., Freer, J., Fricke, G.M., Galle, B., Gerdes, G., Giudice, G., Gutmann, A., Hayer, C., Itikarai, I., Jones, J., Mason, E., McCormick Kilbride, B.T., Mulina, K., Nowicki, S., Rahilly, K., Richardson, T., Rüdiger, J., Schipper, C.I., Watson, I.M., Wood, K., Moor, J.M., Diaz, J.A., Edmonds, M., Fischer, T.P., Freer, J., Fricke, G.M., Galle, B., Gerdes, G., Giudice, G., Gutmann, A., Hayer, C., Itikarai, I., Jones, J., Mason, E., Kilbride, B.T.M., Mulina, K., Nowicki, S., Rahilly, K., Richardson, T., Rüdiger, J., Schipper, C.I., Watson, I.M., Wood, K., 2020. Aerial strategies advance gas measurements at inaccessible, strongly degassing volcanoes. *Sci. Adv.* 6, eabb9103.
- Lopez, T., Aguilera, F., Tassi, F., Maerten de Moor, J., Bobrowski, N., Aiuppa, A., Tamburello, G., Rizzo, A.L., Liuzzo, M., Viveiros, F., Cardellini, C., Silva, C., Fischer, T., Jean-Baptiste, P., Kazayaha, R., Hidalgo, S., Malowany, K., Lucic, G., Bagnato, E., Bergsson, B., Reath, K., Liotta, M., Carn, S., Chiodini, G., 2018. New insights into the magmatic-hydrothermal system and volatile budget of Lastarria volcano, Chile: Integrated results from the 2014 IAVCEI CCVG 12th Volcanic Gas Workshop. *Geosphere* 14, 983–1007. <https://doi.org/10.1130/GES01495.1>.
- Martin, C.R., Zeng, N., Karion, A., Dickerson, R.R., Ren, X., Turpie, B.N., Weber, K.J., 2017. Evaluation and environmental correction of ambient CO<sub>2</sub> measurements from a low-cost NDIR sensor. *Atmos. Meas. Tech.* 10, 2383–2395. <https://doi.org/10.5194/AMT-10-2383-2017>.
- Mishra, G.K., Barfidokht, A., Tehrani, F., Mishra, R.K., 2018. Food safety analysis using electrochemical biosensors. *Foods* 7, 141. <https://doi.org/10.3390/FOODS7090141>.
- Padrón, E., Hernández, P.A., Pérez, N.M., Toulkeridis, T., Melián, G., Barrancos, J., Virgili, G., Sumino, H., Notsu, K., 2012. Fumarole/plume and diffuse CO<sub>2</sub> emission from Sierra Negra caldera, Galapagos archipelago. *Bull. Volcanol.* 74, 1509–1519. <https://doi.org/10.1007/S00445-012-0610-4/TABLES/3>.
- Pering, T.D., Tamburello, G., McGonigle, A.J.S., Aiuppa, A., Cannata, A., Giudice, G., Patané, D., 2014. High time resolution fluctuations in volcanic carbon dioxide degassing from Mount Etna. *J. Volcanol. Geotherm. Res.* 270, 115–121. <https://doi.org/10.1016/j.jvolgeores.2013.11.014>.
- Pering, T.D., Liu, E.J., Wood, K., Wilkes, T.C., Aiuppa, A., Tamburello, G., Bitetto, M., Richardson, T., McGonigle, A.J.S., 2020. Combined ground and aerial measurements resolve vent-specific gas fluxes from a multi-vent volcano. *Nat. Commun.* 11, 3039. <https://doi.org/10.1038/s41467-020-16862-w>.
- Roberts, T.J., Braban, C.F., Oppenheimer, C., Martin, R.S., Freshwater, R.A., Dawson, D. H., Griffiths, P.T., Cox, R.A., Saffell, J.R., Jones, R.L., 2012. Electrochemical sensing of volcanic gases. *Chem. Geol.* 332–333, 74–91. <https://doi.org/10.1016/J.CHEMGEO.2012.08.027>.
- Roberts, T.J., Saffell, J.R., Oppenheimer, C., Lurton, T., 2014. Electrochemical sensors applied to pollution monitoring: Measurement error and gas ratio bias – a volcano

- plume case study. *J. Volcanol. Geotherm. Res.* 281, 85–96. <https://doi.org/10.1016/J.JVOLGEORES.2014.02.023>.
- Roberts, T.J., Lurton, T., Giudice, G., Liuzzo, M., Aiuppa, A., Coltelli, M., Vignelles, D., Salerno, G., Couté, B., Chartier, M., Baron, R., Saffell, J.R., Scaillet, B., 2017. Validation of a novel multi-gas sensor for volcanic HCl alongside H<sub>2</sub>S and SO<sub>2</sub> at Mt. Etna 79, 1–14.
- Roberts, T.J., Vignelles, D., Liuzzo, M., Giudice, G., Aiuppa, A., Coltelli, M., Salerno, G., Chartier, M., Couté, B., Berthet, G., Lurton, T., Dulac, F., Renard, J.B., 2018. The primary volcanic aerosol emission from Mt Etna: Size-resolved particles with SO<sub>2</sub> and role in plume reactive halogen chemistry. *Geochim. Cosmochim. Acta* 222, 74–93. <https://doi.org/10.1016/J.GCA.2017.09.040>.
- Rüdiger, J., Tirpitz, J.L., Maarten De Moor, J., Bobrowski, N., Gutmann, A., Liuzzo, M., Ibarra, M., Hoffmann, T., 2018. Implementation of electrochemical, optical and denuder-based sensors and sampling techniques on UAV for volcanic gas measurements: examples from Masaya, Turrialba and Stromboli volcanoes. *Atmos. Meas. Tech.* 11, 2441–2457. <https://doi.org/10.5194/AMT-11-2441-2018>.
- Saini, J., Dutta, M., Marques, G., 2021. Indoor Air Quality and internet of things: the State of the Art. *SpringerBriefs Appl. Sci. Technol.* 33–50 [https://doi.org/10.1007/978-3-030-82216-3\\_3/COVER](https://doi.org/10.1007/978-3-030-82216-3_3/COVER).
- Sajjan, V., Sharma, P., 2021. Analysis of air pollution by using raspberry Pi-IoT. In: *Proc. 6th Int. Conf. Inven. Comput. Technol.*, 2021. ICICT, pp. 178–183. <https://doi.org/10.1109/ICICT50816.2021.9358535>.
- Salas-Navarro, J., Stix, J., de Moor, J.M., 2022. A new Multi-GAS system for continuous monitoring of CO<sub>2</sub>/CH<sub>4</sub> ratios at active volcanoes. *J. Volcanol. Geotherm. Res.* 107533 <https://doi.org/10.1016/J.JVOLGEORES.2022.107533>.
- Shinohara, H., 2005. A new technique to estimate volcanic gas composition: Plume measurements with a portable multi-sensor system. *J. Volcanol. Geotherm. Res.* 143, 319–333. <https://doi.org/10.1016/j.jvolgeores.2004.12.004>.
- Stix, J., de Moor, J.M., Rüdiger, J., Alan, A., Corrales, E., D'Arcy, F., Diaz, J.A., Liotta, M., 2018. Using Drones and Miniaturized Instrumentation to Study Degassing at Turrialba and Masaya Volcanoes, Central America. *J. Geophys. Res. Solid Earth* 123, 6501–6520. <https://doi.org/10.1029/2018JB015655>.
- Symonds, R.B., Gerlach, T.M., Reed, M.H., 2001. Magmatic gas scrubbing: implications for volcano monitoring. *J. Volcanol. Geotherm. Res.* 108, 303–341. [https://doi.org/10.1016/S0377-0273\(00\)00292-4](https://doi.org/10.1016/S0377-0273(00)00292-4).
- Tainio, M., Jovanovic Andersen, Z., Nieuwenhuijsen, M.J., Hu, L., de Nazelle, A., An, R., García, L.M.T., Goenka, S., Zapata-Diomedí, B., Bull, F., Sá, T.H., 2021. Air pollution, physical activity and health: a mapping review of the evidence. *Environ. Int.* 147, 105954 <https://doi.org/10.1016/J.ENVINT.2020.105954>.
- Tamburello, G., 2015. Ratiocalc: Software for processing data from multicomponent volcanic gas analyzers. *Comput. Geosci.* 82, 63–67. <https://doi.org/10.1016/J.CAGEO.2015.05.004>.
- Tamburello, G., Hansteen, T.H., Bredemeyer, S., Aiuppa, A., Tassi, F., 2014. Gas emissions from five volcanoes in northern Chile and implications for the volatiles budget of the Central Volcanic Zone. *Geophys. Res. Lett.* 41, 4961–4969. <https://doi.org/10.1002/2014GL060653>.
- Tassi, F., Aguilera, F., Vaselli, O., Darrah, T., Medina, E., 2011. Gas discharges from four remote volcanoes in northern Chile (Putana, Olca, Irruputuncu and Alitar): a geochemical survey. *Ann. Geophys.* 54 (2) <https://doi.org/10.4401/ag-5173>.
- Unera, D.M., Tobón, D.P., Aguirre, J., Gaviria Gómez, N., Múnera, D., 2021. IoT-based air quality monitoring systems for smart cities: a systematic mapping study. *Int. J. Electr. Comput. Eng.* 11, 3470–3482. <https://doi.org/10.11591/ijece.v11i4.pp3470-3482>.
- Vallero, D., 2014. *Fundamentals of Air Pollution*, 5th ed. Eksevier, Oxford.
- Villa, T.F., Salimi, F., Morton, K., Morawska, L., Gonzalez, F., 2016. development and validation of a uav based system for air pollution measurements. *Sensors* 16, 2202. <https://doi.org/10.3390/S16122202>.
- Wang, Y., Xu, H., Zhang, J., Li, G., 2008. Electrochemical sensors for clinic analysis. *Sensors* 8, 2043–2081. <https://doi.org/10.3390/S8042043>.
- Wang, P., Mihaylova, L., Chakraborty, R., Munir, S., Mayfield, M., Alam, K., Khokhar, M. F., Zheng, Z., Jiang, C., Fang, H., 2021. A Gaussian process method with uncertainty quantification for air quality monitoring. *Atmos* 12, 1344. <https://doi.org/10.3390/ATMOS12101344>.
- Werner, C., Fischer, T.P., Aiuppa, A., Edmonds, M., Cardellini, C., Carn, S., Chiodini, G., Cottrell, E., Burton, M., Shinohara, H., Allard, P., 2019. Carbon dioxide emissions from subaerial volcanic regions. In: Orcutt, B.N., Daniel, I., Dasgupta, R. (Eds.), *Deep Carbon: Past to Present*. Cambridge University Press, Cambridge, pp. 188–236.
- Whitty, R.C.W., Pfeffer, M.A., Ilyinskaya, E., Roberts, T.J., Schmidt, A., Barsotti, S., Strauch, W., Crilley, L.R., Pope, F.D., Bellanger, H., Mendoza, E., Mather, T.A., Liu, E.J., Peters, N., Taylor, I.A., Francis, H., Hernández Leiva, X., Lynch, D., Norbert, S., Baxter, P., 2022. Assessing the effectiveness of low-cost air quality monitors for identifying volcanic SO<sub>2</sub> and PM downwind from Masaya volcano, Nicaragua. *Volcanica* 5, 33–59. <https://doi.org/10.30909/VOL.05.01.3359>.
- Wilkes, T., McGonigle, A., Pering, T., Taggart, A., White, B., Bryant, R., Willmott, J., Wilkes, T.C., McGonigle, A.J.S., Pering, T.D., Taggart, A.J., White, B.S., Bryant, R.G., Willmott, J.R., 2016. Ultraviolet imaging with low cost smartphone sensors: development and application of a raspberry Pi-based UV camera. *Sensors* 16, 1649. <https://doi.org/10.3390/s16101649>.
- Wilkes, T., Pering, T., McGonigle, A., Tamburello, G., Willmott, J., Wilkes, T.C., Pering, T.D., McGonigle, A.J.S., Tamburello, G., Willmott, J.R., 2017. A low-cost smartphone sensor-based UV camera for volcanic SO<sub>2</sub> emission measurements. *Remote Sens.* 9, 27. <https://doi.org/10.3390/rs9010027>.
- Wood, K., Liu, E.J., Richardson, T., Clarke, R., Freer, J., Aiuppa, A., Giudice, G., Bitetto, M., Mulina, K., Itikarai, L., 2020. BVLOS UAS operations in highly-turbulent volcanic plumes. *Front. Robot. AI* 7, 136. <https://doi.org/10.3389/FROBT.2020.549716/BIBTEX>.
- Zhang, H., Srinivasan, R., 2020. A systematic review of air quality sensors, guidelines, and measurement studies for indoor air quality management. *Sustain* 12, 9045. <https://doi.org/10.3390/SU12219045>.
- Zhang, H., Srinivasan, R., Ganesan, V., 2021. Low cost, multi-pollutant sensing system using raspberry Pi for indoor air quality monitoring. *Sustain* 13, 370. <https://doi.org/10.3390/SU13010370>.